

### **OPEN ACCESS**

EDITED BY Bin Wang, Shaoguan University, China

REVIEWED BY
Felipe Javier Renna,
National Scientific and Technical Research
Council (CONICET), Argentina
Bin Huai,
Guangdong Academy of Sciences, China

\*CORRESPONDENCE Li Wang ⊠ mirror0117@126.com

RECEIVED 28 July 2025 ACCEPTED 29 September 2025 PUBLISHED 16 October 2025

### CITATION

Ma M, Jiang X, Liu W, Xue J, Yuan Y, Zhi X, Feng J, Long Y, Li Y, Zhang Z, Wang X and Wang L (2025) Quercetin reverses  $\beta_1$ -adrenoceptor autoantibody-induced heart failure by promoting MDM2-mediated ubiquitination and degradation of p53 in cardiomyocytes. Front. Nutr. 12:1674507. doi: 10.3389/fnut.2025.1674507

### COPYRIGHT

© 2025 Ma, Jiang, Liu, Xue, Yuan, Zhi, Feng, Long, Li, Zhang, Wang and Wang. This is an open-access article distributed under the terms of the Creative Commons Attribution License (CC BY). The use, distribution or reproduction in other forums is permitted, provided the original author(s) and the copyright owner(s) are credited and that the original publication in this journal is cited, in accordance with accepted academic practice. No use, distribution or reproduction is permitted which does not comply with these terms

# Quercetin reverses $\beta_1$ -adrenoceptor autoantibody-induced heart failure by promoting MDM2-mediated ubiquitination and degradation of p53 in cardiomyocytes

Mingxia Ma<sup>1</sup>, Xintai Jiang<sup>1</sup>, Weiqian Liu<sup>1</sup>, Jin Xue<sup>1</sup>, Yuan Yuan<sup>2</sup>, Xiaoyan Zhi<sup>1</sup>, Jiayan Feng<sup>1</sup>, Yaolin Long<sup>1</sup>, Yang Li<sup>1</sup>, Zhijun Zhang<sup>3</sup>, Xiaohui Wang<sup>1,2</sup> and Li Wang<sup>1,\*</sup>

<sup>1</sup>Department of Pathology, Shanxi Medical University, Taiyuan, Shanxi, China, <sup>2</sup>Morphology Laboratory, Shanxi Medical University, Taiyuan, Shanxi, China, <sup>3</sup>Department of Cardiology, Shanxi Bethune Hospital, Shanxi Academy of Medical Sciences, Third Hospital of Shanxi Medical University, Tongji Shanxi Hospital, Taiyuan, China

**Introduction:** Cardiomyocyte autophagy is essential for preserving cardiac homeostasis. Previous studies revealed that  $\beta_1$ -adrenergic receptor autoantibody ( $\beta_1$ -AA) suppressed cardiomyocyte autophagy, triggering cell death and heart failure (HF). Qiliqiangxin capsule enhances autophagy and mitigates HF through multiple pathways, but its complex composition complicates mechanistic clarity. Network pharmacology identified quercetin as a pivotal autophagy-inducing component in Qiliqiangxin, yet its role in counteracting  $\beta_1$ -AA-induced autophagy impairment remains unvalidated. In this study, quercetin's therapeutic potential and mechanisms in restoring autophagy in  $\beta_1$ -AA-associated HF were investigated.

**Methods:** Bioinformatics methods, including a STRING database analysis, PPI network construction, and Cytoscape-based pathway mapping, were used to delineate quercetin's autophagy-related targets. The *in vivo* efficacy was assessed in  $\beta_1$ -AA-positive mice treated with quercetin (100 mg/[kg·d], intraperitoneal). The *in vitro* validation used H9c2 cardiomyocytes pretreated with quercetin (100  $\mu$ M) prior to  $\beta_1$ -AA exposure. Autophagy markers, p53 signaling, and ubiquitination pathways were analyzed by immunoblotting and functional enrichment analysis using the GOrilla database. A p53 knockdown and overexpressing cardiomyocyte model confirmed pathway specificity.

**Results:** Quercetin administration significantly restored myocardial autophagy levels in  $\beta_1$ -AA-positive mice, which improved cardiac function and survival rates. In H9c2 cells, quercetin pretreatment reversed  $\beta_1$ -AA-induced autophagy suppression. Bioinformatics linked quercetin to p53 pathway modulation, with experimental validation showing quercetin downregulated p53 expression via MDM2-mediated ubiquitination. p53 knockdown enhanced autophagy, while its overexpression blocked quercetin's effect, indicating quercetin restores autophagy in a p53-dependent manner. GO enrichment highlighted the association between quercetin and ubiquitin-dependent protein degradation,

which was corroborated by elevated MDM2 levels and accelerated p53 degradation in quercetin-treated cells.

**Discussion:** Quercetin rescues  $\beta_1$ -AA-impaired cardiomyocyte autophagy by activating MDM2-dependent p53 ubiquitination and degradation, thereby attenuating HF progression. These findings establish quercetin as the mechanistic basis of the cardioprotective effects of Qiliqiangxin and provide preclinical evidence for targeting autophagy by regulating p53 in  $\beta_1$ -AA-induced cardiac dysfunction.

KEYWORDS

heart failure, β<sub>1</sub>-adrenoceptor autoantibody, autophagy, ubiquitination, quercetin

### 1 Introduction

Heart failure, often the terminal stage of various cardiovascular diseases, continues to be a major clinical challenge despite significant progress in therapeutic approaches. Even with treatment, a considerable proportion of patients still suffer from persistent symptoms, with high rates of hospital re-admission and mortality due to disease progression (1). Therefore, identifying targeted pharmacological therapies for heart failure (HF) remains a critical need in the field of cardiovascular research.

Our previous research found that  $\beta_1$ -adrenergic receptor autoantibody ( $\beta_1$ -AA) inhibited autophagy levels in cardiomyocytes, leading to HF (2).  $\beta_1$ -AA is an autoantibody directed against the second extracellular loop (ECII) of the  $\beta_1$ -adrenergic receptor ( $\beta_1$ -AR). Clinical investigations have reported its presence in the serum of approximately 40–60% of patients with HF (3). Removing  $\beta_1$ -AA from patients' blood using immunoadsorption has significantly improved cardiac function, suggesting a close relationship between  $\beta_1$ -AA and HF (4, 5). Although rapamycin-induced upregulation of autophagy levels in cardiomyocytes has effectively improved  $\beta_1$ -AA-induced myocardial injury and dysfunction (2), the clinical use of rapamycin as an immunosuppressant is associated with significant side effects, including the risk of severe infections and death (6). Therefore, identifying safe and effective drugs to upregulate cardiomyocyte autophagy is crucial for improving  $\beta_1$ -AA-induced HF.

An increasing amount of evidence suggests that traditional Chinese medicine is both safe and effective as a HF treatment (7). The Chinese guidelines for chronic HF treatment highlight Qiliqiangxin capsule as an effective therapy for HF (8, 9). Qiliqiangxin capsule is a compound herbal medicine consisting of 11 ingredient plants: Panax ginseng, Astragalus, Rhizoma aconiti lateralis radix preparata, Alisma, Salvia miltiorrhiza, Carthami flos, Semen descurainiae lepidii, Cinnamomi ramulus, Citri reticulatae pericarpium, Polygonati odorati rhizome, and Cortex Periplocae (10). Some studies reported that Qiliqiangxin capsule exhibited protective effects on the heart in HF patients (9, 11, 12), but the specific mechanisms are not clear. In this study, quercetin was identified through network pharmacology analysis as the key component of Qiliqiangxin capsule promoting autophagy. Quercetin is present in multiple herbal components of Qiliqiangxin capsules, with Astragalus, Carthami flos and Semen descurainiae lepidii being the main botanical sources. As a flavonoid that is widely distributed in nature, quercetin enhances mitophagy via the SIRT1/TMBIM6 pathway, thereby improving mitochondrial function and protecting cardiomyocytes (12). Quercetin was also found to regulate miR-223-3p/FOXO3 axis to promote autophagy and suppress isoproterenol-induced myocardial fibrosis (13). Despite promising indications, the potential of quercetin to reverse the  $\beta_1$ -AA-induced autophagy decline and its underlying mechanisms remain unclear. This study combined bioinformatics and molecular biology methods to investigate the molecular mechanisms by which quercetin reverses  $\beta_1$ -AA-induced autophagy suppression and improves HF in mice, providing experimental evidence for the therapeutic potential of quercetin in autophagy-related cardiovascular diseases.

### 2 Materials and methods

### 2.1 Data collection and processing

Microarray data for HF were obtained from the Gene Expression Omnibus (GEO) database (including GSE57338, GSE5406 and GSE3586). The datasets were merged using the R package in SilicoMerging (14), and batch effects were corrected with the Empirical Bayes method proposed by Johnson et al. (15). A differential expression analysis of the data was conducted using the limma R package (version 3.40.6) (16) to identify differentially expressed genes (DEGs). A gene set enrichment analysis of the DEGs was performed using the R package clusterProfiler (version 3.14.3) (17).

# 2.2 Screening of active ingredients in Qiligiangxin capsule

The active ingredient candidate components of Qiliqiangxin capsule were obtained from the TCMSP,¹ which is a valuable tool for investigating the pharmacological mechanisms underlying traditional Chinese medicine (18). Oral bioavailability (OB) refers to the fraction of a drug that reaches systemic circulation, reflecting the absorption rate of active pharmaceutical ingredients. Pharmacokinetic studies are used to determine OB, with higher values indicating better absorption (19). Druglikeness (DL) assesses a small molecule's potential as an orally bioavailable drug. Researchers have suggested that molecules with OB  $\geq$  30% or DL  $\geq$  0.18 have enhanced pharmacological effects (20). Therefore, in this study, the screening criteria for active

<sup>1</sup> https://old.tcmsp-e.com/index.php

ingredients in Qiliqiangxin capsule were defined as compounds meeting both OB  $\geq$  30% and DL  $\geq$  0.18 thresholds.

### 2.3 Screening of target genes for HF

Target genes associated with HF were downloaded from the TTD<sup>2</sup> (21), DisGeNET<sup>3</sup> (22), and DrugBank<sup>4</sup> (23) databases. The datasets from these three databases were integrated by taking their union to obtain a consolidated set of HF-related target genes.

# 2.4 Construction of the HF-target gene-active ingredient network

To elucidate the multi-scale relationships among the active ingredients of Qiliqiangxin capsule, HF-related targets and autophagy-related targets, we constructed an HF-target gene-active ingredient network. The active ingredients and their corresponding targets were derived from the screening process described in Section 2.2, while the HF-related genes were sourced from the databases listed in Section 2.3. A Venn diagram was used to identify the intersection of three specific gene sets: the targets of the active ingredients of Qiliqiangxin capsule, HF-related genes and autophagy-related genes. These overlapping genes were considered potential key targets through which Qiliqiangxin capsule exerts its therapeutic effects on HF by regulating autophagy. The tripartite network was visualized using Cytoscape (v3.7.2) (24). The network consists of nodes representing active ingredients, overlapping target genes, and HF, connected by edges that depict their interactions.

### 2.5 Construction of protein–protein interaction network

We conducted a protein–protein interaction (PPI) analysis using the STRING database,<sup>5</sup> setting the species to "*Homo sapiens*" and applying a score threshold of >0.4 (25). The MCC method of the CytoHubba plugin in Cytoscape (24) was used to identify 10 key targets within the PPI network.

### 2.6 Molecular docking simulation

The MDM2 protein structure was retrieved from the RCSB PDB database<sup>6</sup> (26), while the molecular structure of quercetin was sourced from the Traditional Chinese Medicine Systems Pharmacology Database (TCMSP) platform. Before docking with AutoDockTools (27), we protonated the molecules and assessed their charge states. Docking was performed using Vina with optimized docking site settings. The results were visualized using PyMOL (28).

- 2 https://db.idrblab.net/ttd/
- 3 https://disgenet.cn
- 4 https://go.drugbank.com/
- 5 https://string-db.org/
- 6 https://www.rcsb.org/

### 2.7 Molecular dynamics simulations

The molecular dynamics simulations were conducted using the academic version of Desmond/Maestro (v2022.1). The simulation systems were solvated using a TIP3P water model and neutralized with 0.15 M sodium chloride solution. Following energy minimization and system equilibration, a 100-ns production run was executed under NPT conditions (300 K, 1 atm). Trajectory snapshots were captured at 100-ps intervals for subsequent analysis. All post-simulation analyses were carried out using a built-in simulation interaction diagram tool in Desmond.

### 2.8 Animal models

Male C57BL/6 mice 6-8 weeks of age were obtained from the Experimental Animal Center of Shanxi Medical University. An active immunization model was generated based on protocols outlined in earlier studies (2, 29). The quercetin monotherapy group and the quercetin treatment group were each administered quercetin (Q4951, Sigma Aldrich) via intraperitoneal injection at a dose of 100 mg/(kg· d) (30) for 4 consecutive weeks after the initial primary immunization. The mice were anesthetized via intraperitoneal injection of sodium pentobarbital at a concentration of 1% in saline, administered at a dose of 40 mg/kg body weight. Blood was drawn from the retroorbital venous plexus of the mice and centrifuged at 3,000 × g for 10 min. Serum  $\beta_1$ -AA concentrations in actively immunized mice were subsequently determined using the SA-ELISA (2, 29, 31) (Supplementary Figure S1). At the end of the experiment, the mice were euthanized by intraperitoneal injection of an overdose of sodium pentobarbital, with death confirmed by cessation of breathing and heartbeat. All animal experiments were performed in strict compliance with the ARRIVE guidelines and relevant regulations, with protocols approved by the Experimental Animal Ethics Committee of Shanxi Medical University (Approval SYDL2024037).

### 2.9 Small animal ultrasound

The echocardiographic analysis primarily included parameters such as left ventricular internal systolic diameter (LVIDs), left ventricular internal diastolic diameter (LVIDd), end-systolic volume (ESV), and end-diastolic volume (EDV), along with reduced ejection fraction (EF) and fractional shortening (FS).

### 2.10 Masson staining

After fixation and dehydration, the cardiac tissue was embedded in paraffin and cut into 5  $\mu m$  sections. Masson staining was performed to examine the histological morphology of the cardiac tissue.

### 2.11 Cell culture and treatments

H9c2 cells (GNR 5) were cultured as described in our previous studies (2, 29). The knockdown efficiency was verified, with the

results presented in Supplementary Figure S2. Stable knockdown clones were selected for subsequent stimulation experiments. The following cell groups were included in the study: the control group (treated with 1  $\mu M$  negative IgG for 24 h), the quercetin group (pretreated with 100  $\mu M$  quercetin for 4 h), the  $\beta_1$ -AA group (treated with 1  $\mu M$   $\beta_1$ -AA for 24 h), the  $\beta_1$ -AA + quercetin group (pretreated with 100  $\mu M$  quercetin for 4 h, then treated with 1  $\mu M$   $\beta_1$ -AA for 24 h), and the p53 knockdown+ $\beta_1$ -AA + quercetin group (In the stably transfected p53 knockdown H9c2 cells, pretreatment with 100  $\mu M$  quercetin was performed for 4 h, followed by treatment with 1  $\mu M$   $\beta_1$ -AA for 24 h).

### 2.12 RNA preparation and RT-Q-PCR

Quantitative PCR was performed using the RT-qPCR rapid qPCR hybrid kit containing TB Green (Takara, RR430A, JPN). The primer sequences can be found in Supplementary Table S1.

### 2.13 Co-immunoprecipitation

Protein A/G magnetic beads were incubated with p53 antibody and rabbit IgG antibody at 4 °C for 6 h, followed by an overnight incubation with protein lysates. The protein was eluted from the beads and denatured before being analyzed by western blotting.

### 2.14 Western blot

Western blot analyses were performed as previously described (29). The antibody catalog numbers are listed in Supplementary Table S2.

### 2.15 Immunofluorescence

Cells were fixed on slides with a 1:1 mixture of methanol and propylene glycol for 15 min, followed by three washes. The cells were blocked with a 5% bovine serum albumin (BSA) solution for 1 h. Next, the cells were incubated with p53 antibody at 4 °C for 16 h, and then with fluorescent secondary antibody at 37 °C for 1 h in the dark. Finally, the slides were mounted with a medium containing DAPI, and immunofluorescence images were captured using a confocal laser scanning microscope.

### 2.16 Plasmid transfection and detection

Sterile cell climbing slices were pre-placed in 12-well plates, and H9c2 cells were seeded at an appropriate density onto the slices and cultured for 24 h. Transfection of GFP-LC3 plasmid was carried out using Lip3.0 reagent (Hanbio Co., Ltd., Shanghai, China) as follows: 4  $\mu g$  of plasmid was added to 250  $\mu L$  of DMEM in a sterile tube and gently mixed; separately, 6  $\mu L$  of LipoFiter3.0 reagent (Hanbio) was mixed with 250  $\mu L$  of Dulbecco's Modified Eagle Medium (DMEM) in another sterile tube and incubated at room temperature for 5 min. The DNA solution was then combined with the LipoFiter3.0 solution,

mixed gently, and incubated at room temperature for 20 min to form complexes. The resulting complexes were added dropwise to the plates containing cell climbing slices. After 6 h of transfection, the medium was replaced with complete medium containing 10% fetal bovine serum (2 mL). At 48 h post-transfection, the cell climbing slices were collected, washed with Phosphate-Buffered Saline (PBS), fixed with 4% paraformaldehyde for 15 min, and permeabilized with 0.1% Triton X-100 for 10 min. The slices were then incubated with 4′,6-diamidino-2-phenylindole (DAPI) staining working solution in the dark for 10 min to label nuclei. After washing three times with PBS, the slices were mounted with antifade mounting medium and observed under a laser scanning confocal microscope to quantify GFP-LC3 puncta and assess nuclear morphology.

### 2.17 Statistical analysis

Student's t-test was used to compare differences between two groups, and one-way ANOVA with Bonferroni  $post\ hoc$  test was used for multiple group comparisons. p < 0.05 was considered statistically significant.

### 3 Results

# 3.1 GEO database analysis revealed significant enrichment of autophagy-related pathways in the myocardial tissue of HF patients

To systematically investigate key pathway alterations in myocardial tissue in the pathogenesis of HF, we integrated three gene expression microarray datasets (GSE5406, GSE57338, GSE3586) derived from human myocardial tissue (Table 1). After batch effect correction and merging the datasets (Figures 1A,B), a cohort consisting of 385 HF patients and 164 healthy controls was constructed. An analysis of the differential expression identified a total of 213 significantly DEGs, with 109 significantly upregulated and 104 significantly downregulated (Figures 1C,D; Supplementary Table S3). To further elucidate the biological functions of these DEGs, a KEGG pathway enrichment analysis was performed. The results demonstrated significant enrichment of autophagy-related pathways, including phagosome, lysosome, mitophagy-animal, and mTOR signaling pathways (Figure 1E). These findings suggested that autophagy dysregulation in myocardial tissue may contribute to human HF.

TABLE 1 The number of sample for HF and normals in include datasets.

Tissue	GSE	platform	HF	Healthy
	GSE57338	Gpl11532	177	136
Lelf ventricle	GSE5406	Gpl125134	193	16
	GSE3586	Gpl1153296	15	12

Sample distribution of HF and Healthy tissues across included datasets from the GEO. The table summarizes the number of samples for each condition (HF and Normal) along with the corresponding GSE accession numbers and platform identifiers for left ventricular cardiac

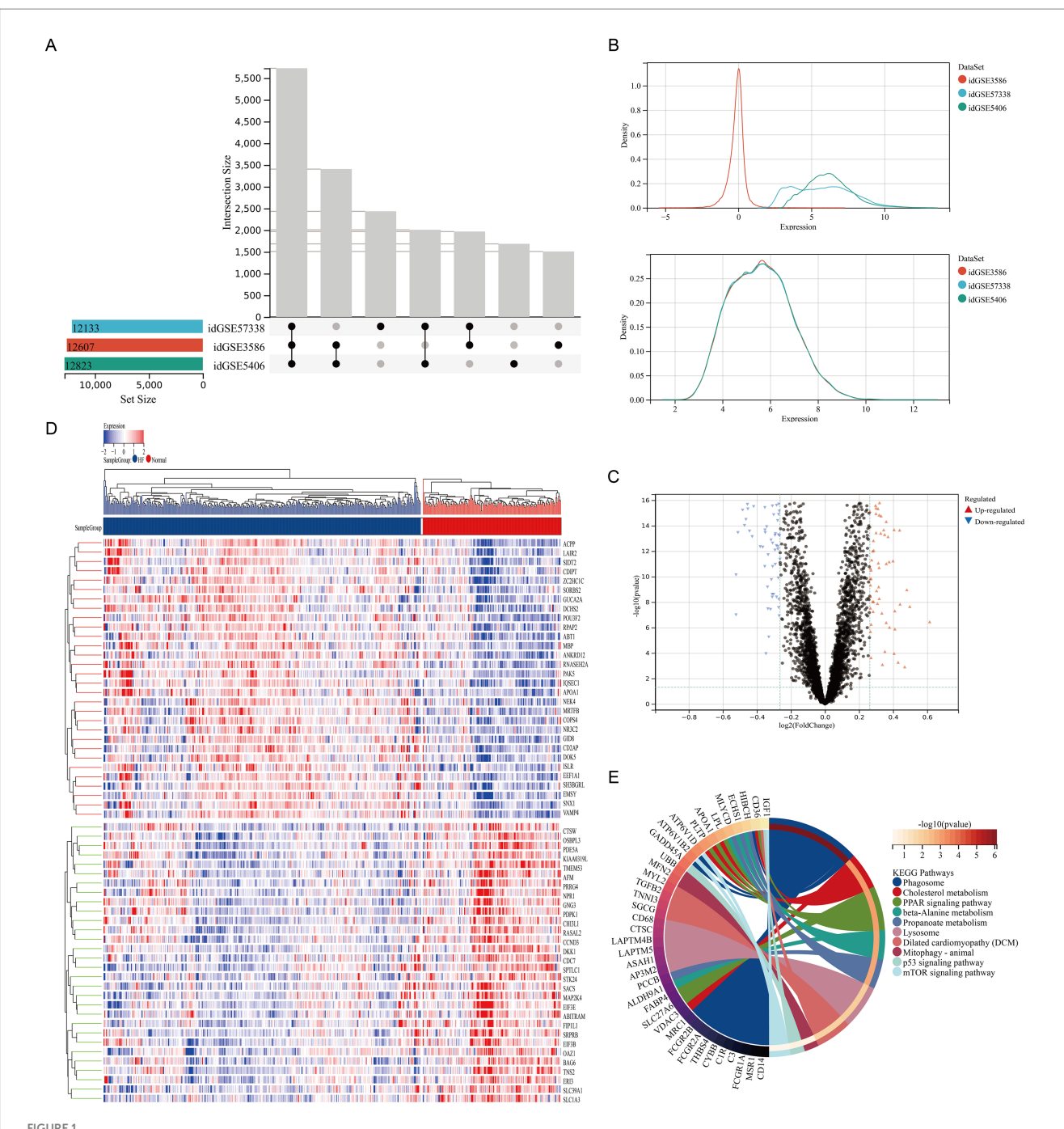
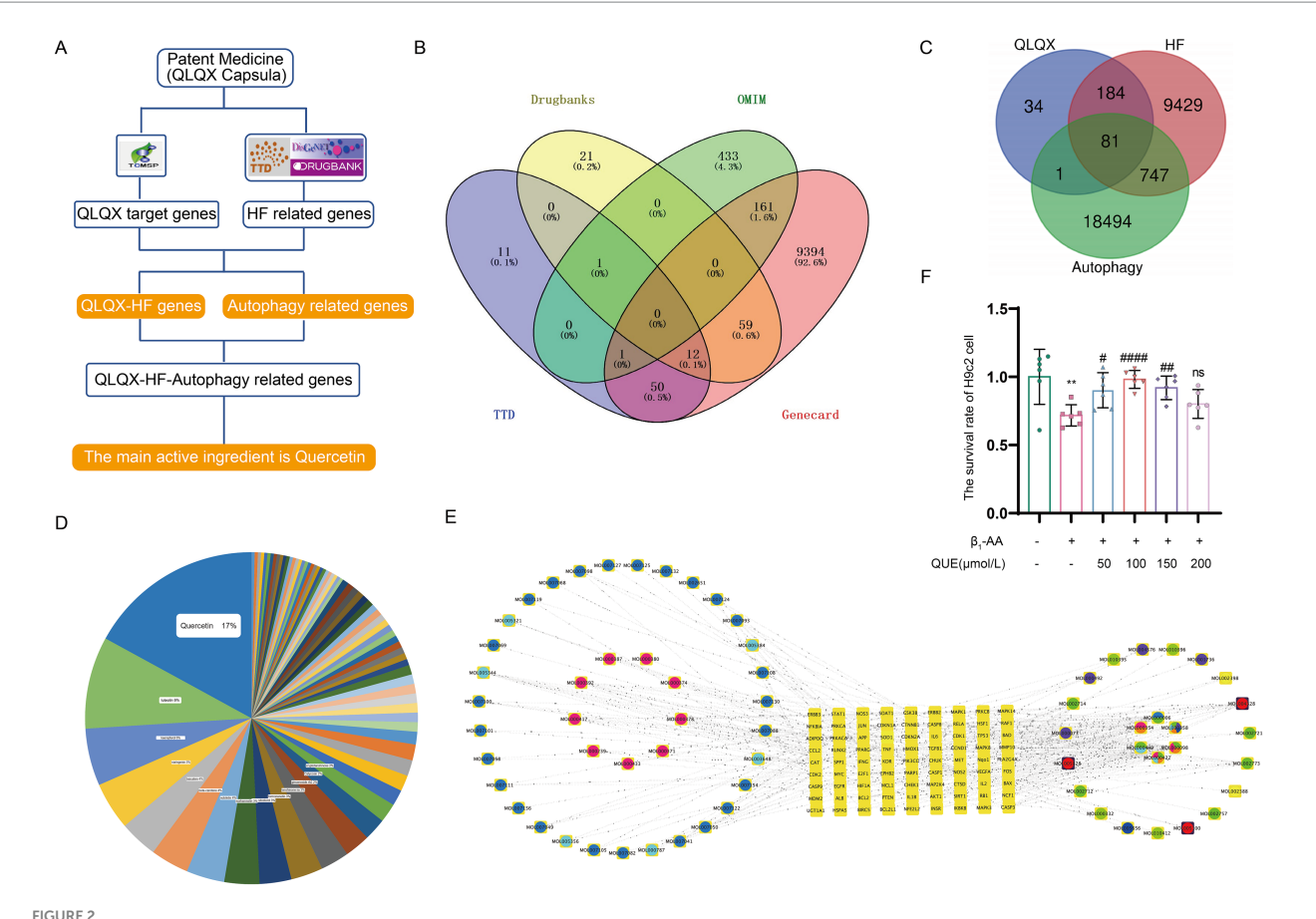


FIGURE 1
GEO database analysis revealed significant enrichment of autophagy-related pathways in the myocardial tissue of HF patients. (A) UpSet plot analysis of three HF datasets. Left bars (X: Set Size) show the total genes per dataset. The main plot (Y: Intersection Size) shows genes shared by specific dataset combinations, with dots representing unique gene counts for the corresponding connected sets below, identifying common and unique genes.
(B) Batch effect correction using an empirical Bayes method. Density distributions of gene expression show multimodal patterns before correction and unimodal patterns after correction (X, gene expression values; Y, probability density). (C) Volcano Plot of DEGs. The plot shows gene expression changes [X:  $\log_2 FC$ ; Y:  $-\log_1 o(a)$ , P-value)]. Red, significantly upregulated genes (p < 0.05,  $\log_2 FC \ge 0.263$ ); gray, non-significantly regulated genes. (D) Heatmap of DEGs showing the expression of significantly differentially expressed genes (adj. p < 0.05,  $\log_2 FC \ge 0.263$ ) across samples. Rows, genes; columns, samples by group. Color gradient, blue (low) to red (high) expression (row Z-score normalized). (E) KEGG enrichment chord plot of DEGs, showing significant pathway-gene interactions (adj. p < 0.05). Outer arc, pathway terms; inner arc, DEGs. Ribbon width indicates enrichment strength; color corresponds to  $-\log_1 o(a)$ , P-value).

# 3.2 Quercetin is a key active component in Qiliqiangxin capsule that upregulates autophagy

In this research, a network pharmacology analysis was performed to identify the key constituents in the traditional Chinese formulation,

Qiliqiangxin capsule, that are responsible for enhancing autophagy (Figure 2A). We used the TCMSP database to obtain the active components and corresponding protein targets (Supplementary Table S4) of the 11 herbs in Qiliqiangxin capsule (Panax ginseng, Astragalus, Rhizoma aconiti lateralis radix preparata, Alisma, Salvia miltiorrhiza, Carthami flos, Semen descurainiae lepidii,



Quercetin is a key active component in Qiliqiangxin capsule autophagy upregulation. (A) Network pharmacology workflow diagram. (B) Integration of HF genes from DrugBank, OMIM, TTD, and GeneCards. (C) The intersection of Qiliqiangxin capsule HF-related targets with autophagy-related genes identified in 81 autophagy-related genes. (D) Chart indicating the proportions of active components in Qiliqiangxin capsule related to HF and autophagy, with quercetin having the highest proportion. (E) Network diagram of traditional Chinese medicine (TCM) active components in Qiliqiangxin capsule related to HF and autophagy. Yellow square nodes represent target genes; red, yellow, green, purple and blue nodes represent TCM herbs; circular nodes represent active components. (F) Effect of quercetin on  $β_1$ -AA-induced H9c2 cardiomyocyte death. Quercetin was tested at concentrations of 50, 100, 150, and 200 μM. The CCK8 assay showed that 100 μM quercetin significantly attenuated  $β_1$ -AA-induced H9c2 cardiomyocyte death (\*\*p < 0.01 vs. Ctrl; "p < 0.05, ""p < 0.001 vs.  $β_1$ -AA group, p = 6).

Cinnamomi ramulus, Citri reticulatae pericarpium, Polygonati odorati rhizome, and Cortex Periplocae). By searching multiple online databases (Disgenet, GeneCards, TTD, and DrugBank), we identified 265 targets related to HF treatment (Figure 2B) from Qiliqiangxin capsule (Supplementary Table S5). To find the targets related to both Qiliqiangxin capsule and autophagy, we intersected the 265 HF-related targets with autophagy-related genes (Figure 2C), which identified 81 autophagy-related genes (Supplementary Table S6). Further analysis of the active components corresponding to these 81 autophagy-related genes revealed that quercetin had the highest proportion (Figures 2D,E). We then explored how quercetin influences cardiomyocyte death mediated by  $\beta_1$ -AA. We tested quercetin at four concentrations: 50, 100, 150, and 200 µM. The results of a CCK8 assay indicated that quercetin at concentrations of 50, 100, and 150 μM mitigated β<sub>1</sub>-AA-induced death of H9c2 cardiomyocytes, with the 100 µM concentration demonstrating a significant protective effect against β<sub>1</sub>-AA-induced H9c2 cardiomyocyte death (Figure 2F).

# 3.3 Quercetin reverses $\beta_1$ -AA-induced myocardial fibrosis and cardiac dysfunction in mice

To evaluate the therapeutic effect of quercetin on  $\beta_1$ -AA-induced HF, an HF phenotype was established in mice through active immunization with  $\beta_1$ -AR-ECII peptide via subcutaneous multi-point injections over a four-week period, with booster immunizations administered every 2 weeks. Concurrently with the modeling, the treatment group received daily intraperitoneal injections of 100 mg/kg quercetin to assess its therapeutic efficacy. To determine the effects of quercetin on cardiac function, we performed echocardiography. We found that the  $\beta_1$ -AA group of mice developed significant cardiac dysfunction, specifically manifested as increased LVIDs, LVIDd, ESV, and EDV, along with reduced EF and FS. Quercetin treatment significantly reversed these abnormal cardiac function indicators (Figures 3A–G), indicating that quercetin exerted a protective effect on cardiac function. We next evaluated myocardial histopathological

changes by analyzing the degree of myocardial fibrosis using Masson staining. The results showed significant collagen deposition in the myocardial interstitium of mice in the  $\beta_1$ -AA group, while quercetin treatment markedly attenuated this pathological fibrotic change (Figures 3J,K). Finally, we measured the mRNA expression of the HF markers Anp and Bnp.  $\beta_1$ -AA significantly upregulated the expression of these two markers, further confirming impaired cardiac function in the model group, whereas quercetin treatment effectively suppressed the increased expression of these markers (Figures 3H,I).

# 3.4 Quercetin reverses $\beta_1$ -AA-induced decrease in myocardial cell autophagy

To investigate the role of autophagy in quercetin-mediated protection against β<sub>1</sub>-AA-induced myocardial injury, key indicators of autophagic flux were systematically evaluated in both in vivo and in vitro models. In the cardiac tissue from  $\beta_1$ -AA-positive mice, intraperitoneal administration of quercetin significantly increased LC3-II protein and LC3 mRNA levels compared to those of the  $\beta_1$ -AA group without quercetin treatment. Quercetin treatment also reduced the accumulation of the autophagy substrate p62 (Figures 4A-C, G). In H9c2 cells, pretreatment with 100 μM quercetin for 4 h prior to 24 h  $\beta_1$ -AA exposure increased LC3-II levels and decreased p62 levels (Figures 4D-F, H). An immunofluorescence analysis revealed a higher number of LC3 puncta in quercetin-pretreated cardiomyocytes following β<sub>1</sub>-AA challenge compared to the β<sub>1</sub>-AA alone group (Figures 4I,J). These results collectively indicate that quercetin enhances autophagic flux and mitigates β<sub>1</sub>-AA-induced impairment of autophagy.

# 3.5 Quercetin reverses the reduction in myocardial cell autophagy induced by $\beta_1$ -AA by decreasing p53 protein expression

To explore the potential targets of quercetin, we used the STRING database to construct a PPI network based on its associated genes and visualized the regulatory network using Cytoscape. The cytoHubba algorithm identified p53 as a key hub gene (Figure 5A). To validate the bioinformatic prediction, we examined p53 protein expression using both in vivo and in vitro models. After 4 weeks of immunization, p53 protein levels were significantly elevated in mouse myocardial tissues, while quercetin treatment markedly suppressed the  $\beta_1$ -AA-induced upregulation of p53 protein (Figures 5B,D) We further confirmed this regulatory relationship in a cell model, which produced consistent results (Figures 5C,E). An immunofluorescence analysis revealed a significant increase in the p53 fluorescence intensity in  $\beta_1$ -AA-treated cells, while quercetin treatment effectively reversed the  $\beta_1$ -AA-induced enhanced signal (Figures 5F,G). We then performed lentivirusmediated p53 knockdown to investigate the role of p53 in autophagy regulation. p53 knockdown attenuated the β<sub>1</sub>-AA-induced decrease in both LC3-II protein and mRNA levels and reduced p62 accumulation (Figures 5H, J-M). To determine whether p53 was essential to quercetin-induced autophagy, we established a p53 overexpression model. In normal cells, quercetin treatment significantly restored autophagy levels; however, this restorative effect of quercetin was markedly attenuated in p53-overexpressing cells (Figures 5I, N-P). These results demonstrate that p53 is indispensable for the regulation of autophagy by quercetin. Notably, while quercetin markedly reduced p53 protein levels in cardiomyocytes, p53 mRNA levels remained unchanged (Figure 5Q), indicating that quercetin may modulate p53 post-transcriptional levels, possibly by promoting its protein degradation.

# 3.6 Quercetin reverses the decrease in p53 ubiquitination levels induced by $\beta_1$ -AA in myocardial cells

To investigate the role of quercetin in p53 degradation, we performed GO functional enrichment analysis of quercetintargeted proteins using R packages (clusterProfiler, org.Hs.eg.db, enrichplot, and ggplot2). The results revealed that quercetin-targeted proteins were significantly enriched in pathways related to ubiquitination (Figure 6A), with similar results obtained through GOrilla database analysis (Supplementary Figure S3). Additionally, H9c2 cardiomyocytes were pretreated with 100  $\mu$ M quercetin for 4 h, followed by treatment with 10  $\mu$ M cycloheximide (CHX) at specified time points. The results demonstrated that quercetin significantly increased the degradation rate of p53 protein (Figures 6B,C). A further analysis of p53 ubiquitination levels indicated that the reduced p53 ubiquitination levels induced by  $\beta_1$ -AA in cardiomyocytes were reversed by quercetin (Figure 6D).

# 3.7 Quercetin reverses the downregulation of MDM2 protein levels in myocardial cells induced by $\beta_1$ -AA

To investigate the mechanism of p53 ubiquitination and degradation, we performed molecular docking to analyze the binding characteristics between the classical E3 ubiquitin ligase MDM2 and quercetin. The results showed that MDM2 binds to quercetin with a binding energy of  $< -6.9 \text{ kcal} \cdot \text{mol}^{-1}$  (Figure 7A), indicating that quercetin effectively targets MDM2. We then conducted molecular dynamics simulations, during which the protein RMSD remained relatively stable, eventually converging between 0.9 and 1.2 Å, while the ligand RMSD stabilized at approximately 3.2 Å after initially fluctuating. This suggested the formation of a more stable binding conformation compared to the initial state (Figure 7B). Next, we analyzed the secondary structure of MDM2. The results revealed that 36.82% of the amino acids were located in  $\alpha$ -helical regions, while 8.60% formed  $\beta$ -strands (Figure 7C). Trajectory plots illustrate the composition of secondary structural elements (SSEs) and the residue distribution per frame (Figure 7D). Compared to disordered regions, these regions are predicted to contribute to more stable binding. Therefore, we evaluated the RMSF of the complex. Residues forming hydrogen bonding (green line) exhibited minimal fluctuations, confirming stable interactions in these regions (Figure 7E). A further analysis of interaction forces and their frequencies in the binding pocket revealed that the interactions were primarily mediated by hydrogen bonds, hydrophobic interactions, and water bridges (Figures 7F,G). The trajectory plots depict the total interactions and specific amino acids involved in each frame (Figure 7H). These results demonstrate that the dynamic interactions between quercetin and

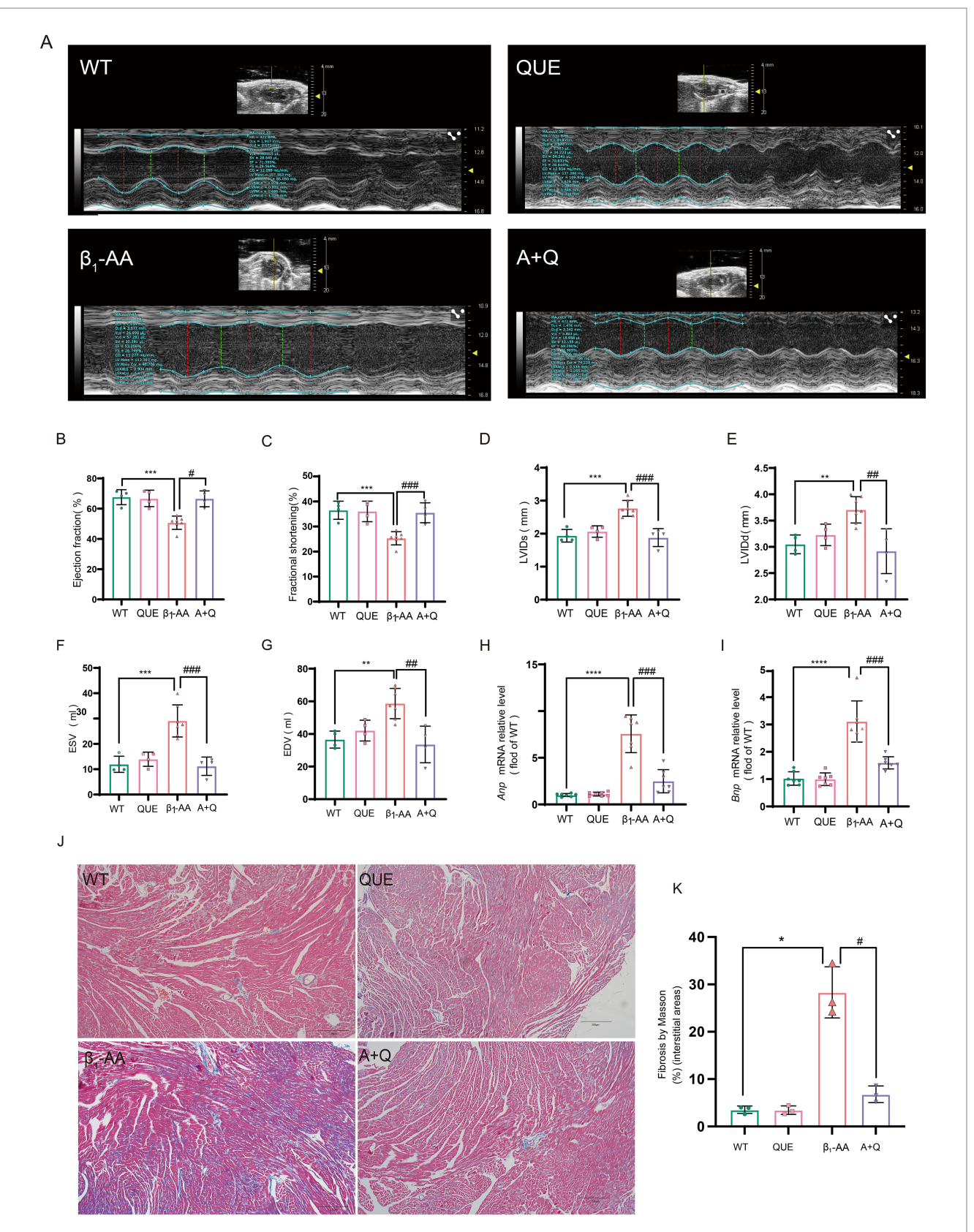


FIGURE 3

Quercetin reverses  $β_1$ -AA-induced cardiac pathological and functional abnormalities in mice. (A–G) Evaluation of EF%, FS%, LVIDd, LVIDs, ESV, and EDV using small animal ultrasound (n = 4-6). (H,I) Quantitative analysis of atrial natriuretic peptide (Anp, n = 6) and brain natriuretic peptide (Bnp, n = 7) mRNA expression in myocardial tissue. (J) Collagen accumulation assessed via Masson's trichrome staining, with collagen fibers indicated in blue. (K) Results of the quantitative analysis of collagen deposition (n = 3). Values are expressed as mean  $\pm$  SD; \*p < 0.05, \*\*p < 0.01, \*\*\*\*p < 0.001, \*\*\*\*p < 0.001, \*\*\*\*p < 0.001 vs. WT; \*p < 0.05, \*\*p < 0.01, \*\*\*\*p < 0.001 vs. B<sub>1</sub>-AA group.

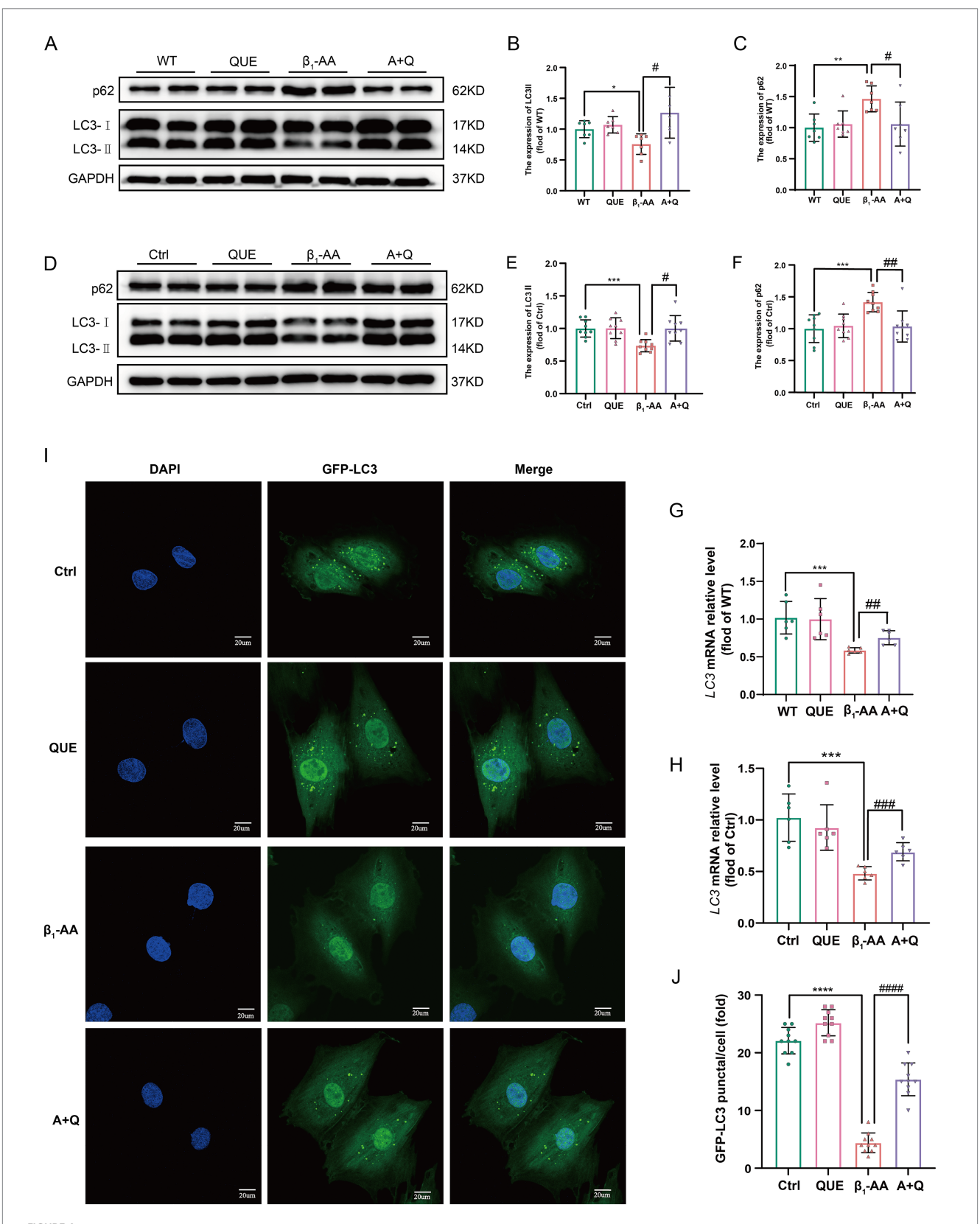


FIGURE 4 Quercetin reverses the decrease in myocardial cell autophagy induced by  $\beta_1$ -AA. (A) Western blot analysis was performed to assess LC3 and p62 protein levels in C57BL/6 mice actively immunized with the  $\beta_1$ -AR-ECII peptide and treated with quercetin for 4 weeks (n=7). (D) Western blot analysis of LC3 and p62 protein levels in H9c2 cardiomyocytes following 24 h of  $\beta_1$ -AA exposure (n=8). (G) LC3 mRNA expression in mice actively immunized with the  $\beta_1$ -AR-ECII peptide for 4 weeks and treated with quercetin, as determined by RT-PCR (n=6). (H) LC3 mRNA expression in H9c2 cells was measured after 24 h of  $\beta_1$ -AA treatment (n=6). (I) Immunofluorescence staining showing LC3 puncta (green fluorescence; scale bar = 20  $\mu$ m).

(Continued)

FIGURE 4 (Continued)

(J) Quantification of LC3 puncta number (n=10). (B,C,E,F) Statistical charts for LC3 and p62. Data are expressed as mean  $\pm$  SD, \*p < 0.05, \*\*p < 0.05, \*\*p < 0.01, \*\*\*p < 0.001 vs. Ctrl or WT; \*p < 0.05, \*\*p < 0.01, \*\*\*p < 0.01 vs. Ctrl or WT; \*p < 0.05, \*\*p < 0.01, \*\*\*p < 0.001 vs.  $p_1 = 0.00$  vs. Ctrl or WT; \*p < 0.05, \*\*p < 0.05, \*\*p < 0.001 vs.  $p_1 = 0.00$  vs. Ctrl or WT; \*p < 0.05, \*\*p < 0.05, \*\*p < 0.001 vs.  $p_1 = 0.00$  vs.  $p_2 = 0.00$  vs.  $p_3 = 0.00$  vs.  $p_3 = 0.00$  vs.  $p_4 = 0.0$ 

MDM2 remained stable over time. Intraperitoneal injection of quercetin significantly reversed the  $\beta_1$ -AA-induced downregulation of MDM2 protein levels in myocardial tissue in the active immunization mouse model, providing experimental validation (Figures 7I,K). After 24 h of  $\beta_1$ -AA treatment, MDM2 protein and mRNA levels were significantly reduced in H9c2 cardiomyocytes, while pre-treatment with quercetin for 4 h markedly increased MDM2 protein (Figures 7J,L) and mRNA levels (Figure 7M). Following treatment with the MDM2-specific inhibitor Nutlin-3a, the effect of quercetin on p53 protein degradation was diminished, and its ability to reverse the  $\beta_1$ -AA-induced decrease in autophagy levels was also weakened (Figures 7N–Q). These findings suggest that quercetin reversed myocardial autophagy by increasing MDM2 protein expression.

### 4 Discussion

Autophagy, vital for maintaining cellular homeostasis and stability under normal physiological conditions, efficiently transports and clears cellular debris, misfolded proteins, and toxic components through lysosomal degradation (32). In cardiac tissue, autophagy is critical for organelle renewal (33). Growing evidence suggests that autophagy is involved in the development of various cardiac diseases, indicating its potential as a therapeutic target for HF. In this study, we performed differential gene expression analysis on the myocardial tissue from HF and non-HF patients using the GEO database. Our findings revealed that DEGs were significantly enriched in autophagy-related pathways. This indicated that modulating autophagy in myocardial cells, either by enhancing or inhibiting its activity, may offer valuable therapeutic means for treating HF (34).

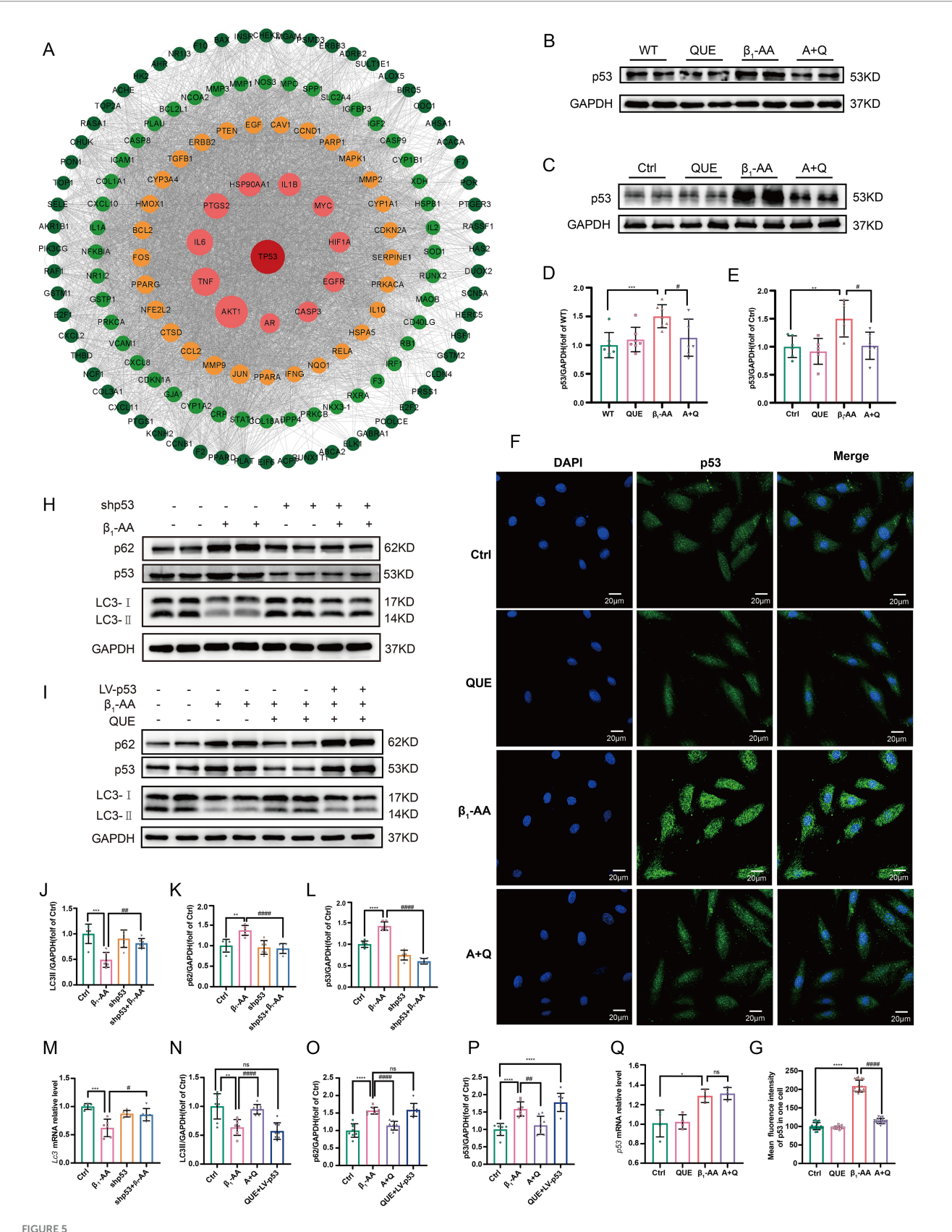
Immune dysfunction is one of the major causes of HF (35). Clinical studies have shown that  $\beta_1$ -AA, a product of immune dysfunction, is present in the serum of patients with dilated cardiomyopathy and HF (31, 36). Overactivation of the  $\beta_1$ -AR is crucial in cardiac hypertrophy and its progression to HF (37, 38). Removing β<sub>1</sub>-AA from patients' blood through immunoadsorption was shown to significantly improve cardiac function (31). Our previous research confirmed that  $\beta_1$ -AA activates the  $\beta_1$ -AR/cAMP/ PKA signaling pathway to suppress cardiomyocyte autophagy (39). Treatment with the autophagy inducer rapamycin to upregulate cardiomyocyte autophagy was shown to significantly improve  $\beta_1$ -AAinduced HF. Therefore,  $\beta_1$ -AA-induced suppression of cardiomyocyte autophagy is a key factor in cardiomyocyte death and cardiac dysfunction (2). However, there is currently a lack of effective drugs that can improve  $\beta_1$ -AA-induced HF. Finding safe and effective drugs that upregulate cardiomyocyte autophagy is crucial for improving  $\beta_1$ -AA-induced HF.

TCM has a history of over 2,000 years, and it is widely used across many countries (40). Increasing research supports the significant safety and efficacy of herbal medicine in treating HF (41). Among these, the Qiliqiangxin capsule, a traditional Chinese medicine, has shown promising results in treating HF (9). This compound herbal

formula contains 11 ingredient plants: Panax ginseng, Astragalus, Rhizoma aconiti lateralis radix preparata, Alisma, Salvia miltiorrhiza, Carthami flos, Semen descurainiae lepidii, Cinnamomi ramulus, Citri reticulatae pericarpium, Polygonati odorati rhizome, and Cortex Periplocae. Studies have demonstrated that Oiligiangxin capsule protected the heart in HF patients (9, 42). It was shown to improve cardiac function in mice post-myocardial infarction by enhancing mitophagy through the Pink1/Parkin signaling pathway (43), and to improve cardiac function in STZ-induced diabetic mice by promoting AGTR1/TRPV1-mediated autophagy (44). Thus, Qiliqiangxin capsule appears to enhance cardiomyocyte autophagy and slow the progression of HF through multiple targets and pathways. However, there is limited research on the precise mechanisms through which Qiliqiangxin capsule exerts its beneficial effects in HF. Network pharmacology is an emerging research method that combines systems biology, genomics, proteomics, and other disciplines to explore drug targets and their molecular mechanisms (45). This method involves virtual computation, high-throughput data analysis, and network database retrieval to elucidate the synergistic effects of multicomponent, multi-channel, and multi-target interactions. Through synergistic multi-component network pharmacology and drug repurposing, precise and effective therapeutic interventions are identified, providing new means of exploring the mechanisms of TCM formulas and accelerating clinical translation. Therefore, in this study, we applied network pharmacology to systematically decipher which natural compounds in Qiliqiangxin capsule improve cardiac function by upregulating cardiomyocyte autophagy. We identified 81 gene targets related to HF, Qiliqiangxin capsule, and autophagy, suggesting that these genes may mediate the decreased autophagy in HF. We constructed an HF-target-active ingredient network, which identified quercetin as the most prominent component of Qiliqiangxin capsule in the treatment of HF.

Quercetin is a polyphenolic flavonoid widely found in fruits and vegetables (46). It is known for its diverse therapeutic effects, including neuroprotection, cardioprotection, and anti-atherosclerotic effects (47). Studies showed that quercetin prevented vascular endothelial dysfunction, reduced end-stage cardiac damage, prevented myocardial fibrosis, and regulated cardiomyocyte redox balance under highglucose conditions. Quercetin was also found to promote desuccinylation of isocitrate dehydrogenase (IDH2) via SIRT5, maintain mitochondrial homeostasis, and alleviate myocardial fibrosis, ultimately reducing the risk of HF (48). Furthermore, quercetin has been shown to enhance mitophagy through the SIRT1/ TMBIM6 pathway, improving mitochondrial energy metabolism and protecting cardiomyocytes (12). Quercetin regulated miR-223-3p/ FOXO3 to promote autophagy and prevent isoproterenol-induced myocardial fibrosis (13). In this study, we similarly observed that quercetin effectively reversed the decline in cardiomyocyte autophagy levels induced by  $\beta_1$ -AA. However, the precise mechanism through which quercetin regulates autophagy requires further exploration.

Further analysis using STRING database, PPI network, and Cytoscape revealed that *p53* is a key target of quercetin. Studies have

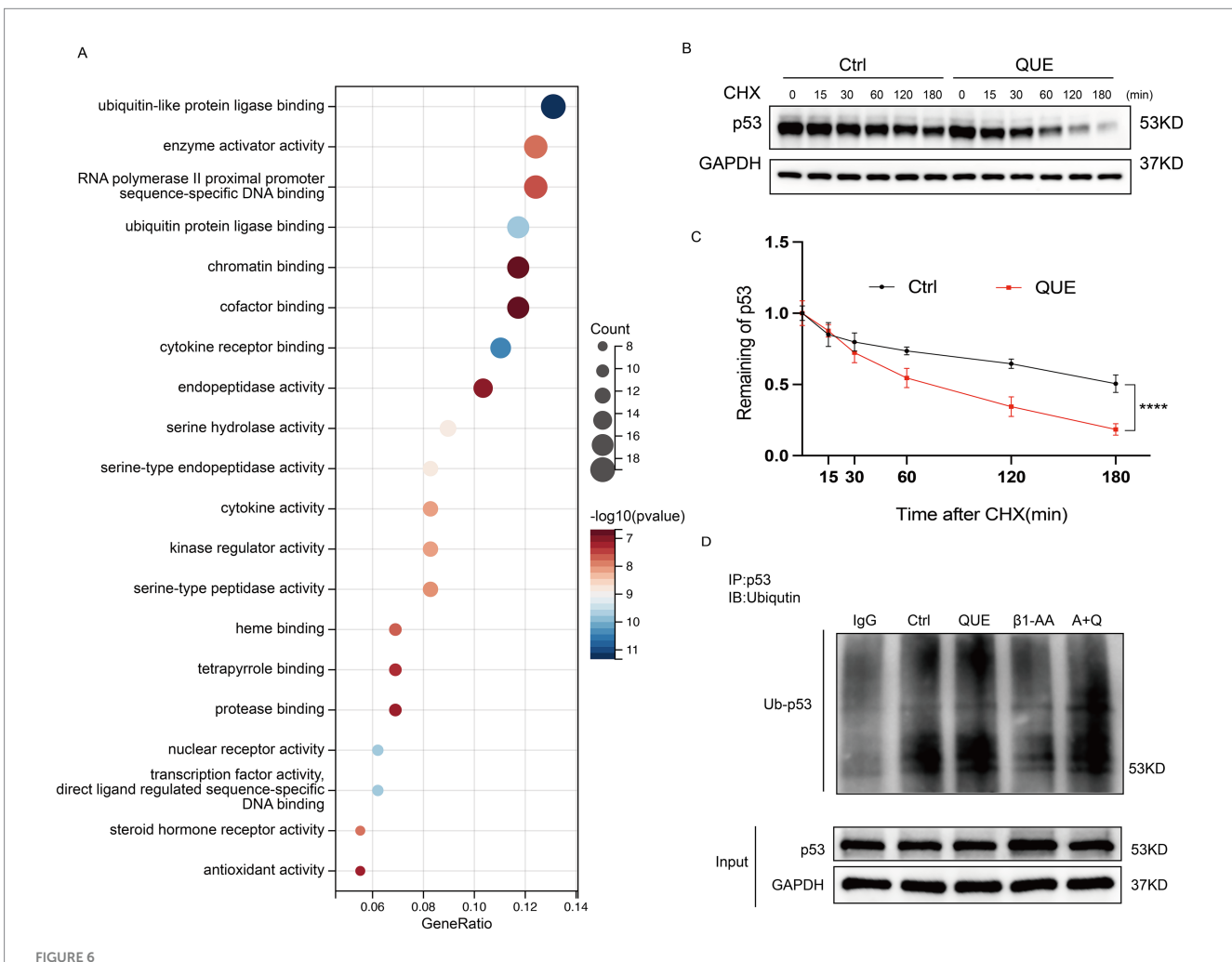


By decreasing p53 protein expression, quercetin reversed the reduction in myocardial cell autophagy induced by  $\beta_1$ -AA. (A) PPI network of quercetin target genes constructed using the STRING database and a regulatory network using Cytoscape. The cytoHubba algorithm identified p53 as a hub gene. (B) Western blot analysis of p53 protein levels in C57BL/6 mice actively immunized with  $\beta_1$ -AR-ECII peptide segment for 4 weeks and treated

(Continued)

#### FIGURE 5 (Continued)

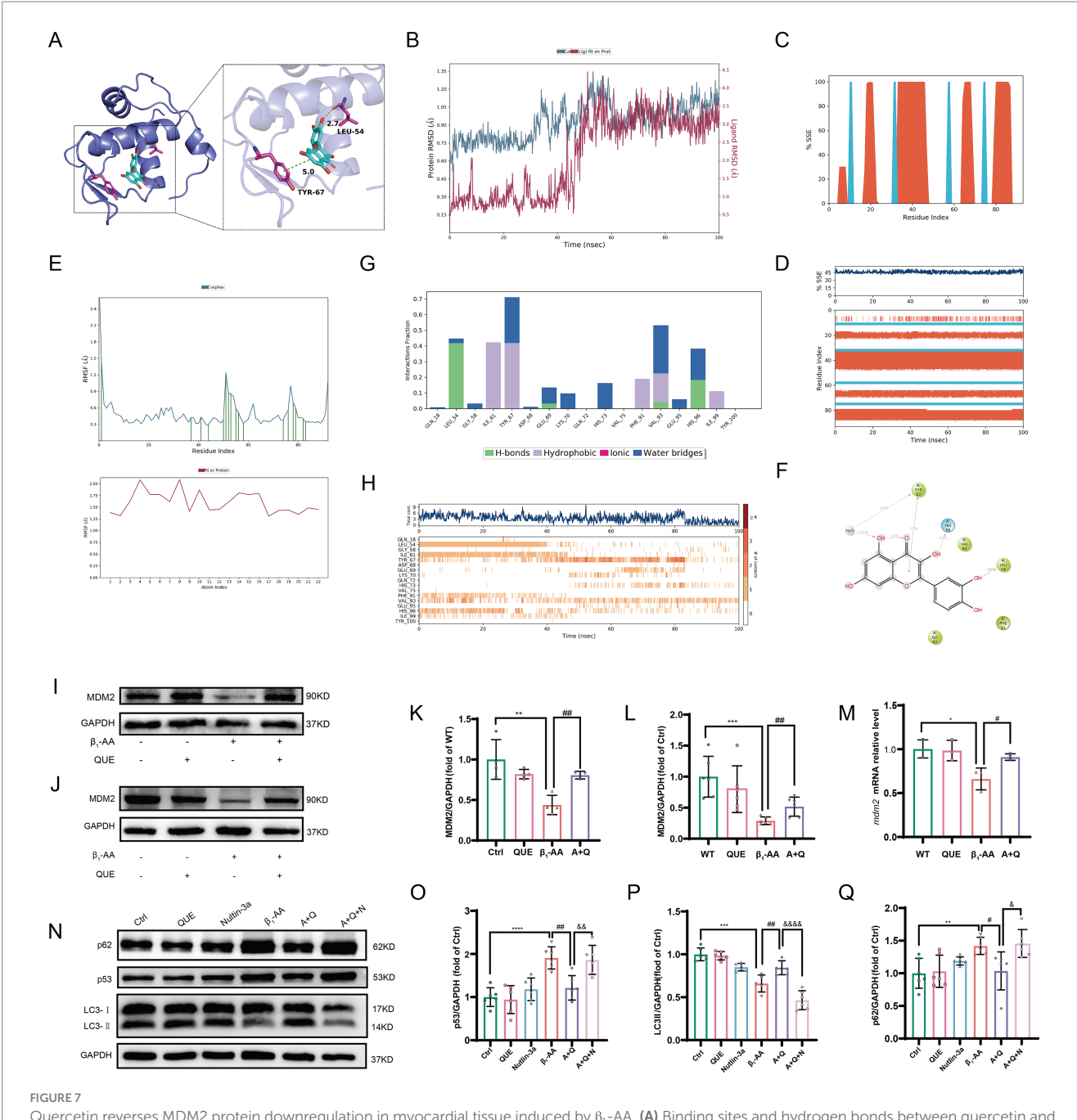
with quercetin (n=7). **(C)** Western blot analysis of p53 protein levels in H9c2 cardiomyocytes after 24 h of  $\beta_1$ -AA treatment (n=6). **(D,E)** Statistical analysis of p53 levels. **(F)** Immunofluorescence detection of p53. Green fluorescence represents p53, scale bar = 20  $\mu$ m. **(G)** Quantification of p53 immunofluorescence intensity. **(H,J,K,L)** Western blot analysis of the protein levels of LC3 and p62 in myocardial cells with lentiviral p53 knockdown and quantified relative protein levels (n=6). **(I,N,O,P)** Western blot analysis of LC3 and p62 protein levels in myocardial cells with p53 overexpression mediated by a lentivirus, and quantification of the relative protein levels (n=6). **(M)** RT-PCR analysis the *LC3* mRNA levels in myocardial cells with p53 knockdown (n=6). **(Q)** The expression level of p53 mRNA in myocardial cells after quercetin treatment. Data are presented as means  $\pm$  SD, \*p < 0.05, \*\*p < 0.01, \*\*\*\*p < 0.001, \*\*\*\*p < 0.001 vs. Ctrl or WT; \*p < 0.05, \*p < 0.05, \*p < 0.05, \*p < 0.001, \*



Quercetin reverses the decrease in p53 ubiquitination levels induced by  $\beta_1$ -AA in myocardial cells. **(A)** GO functional enrichment analysis of quercetin-targeted proteins using the R packages clusterProfiler, org. Hs.eg.db, enrichplot, and ggplot2. **(B)** H9c2 cardiomyocytes were pretreated with 100  $\mu$ M quercetin for 4 h, followed by treatment with 10  $\mu$ M CHX for the specified durations. Cells were analyzed by Western blotting using GAPDH as an internal control. **(C)** Quantitative analysis of protein expression levels (n=4). Data are presented as mean  $\pm$  SD. Statistical significance was determined by two-way ANOVA with Bonferroni's multiple comparison test. \*\*\*\*p<0.0001. **(D)** Co-immunoprecipitation (Co-IP) results show that compared to the control group,  $\beta_1$ -AA treatment reduced p53 ubiquitination levels in myocardial cells, which was significantly reversed by quercetin.

shown that p53 in the cytoplasm acts as an inhibitor of autophagy. In humans, mice, and nematodes, knockout or pharmacological inhibition of p53 has been shown to induce autophagy (49). The results of this study demonstrated that  $\beta_1$ -AA stimulation significantly increased p53 protein levels in cardiomyocytes, which were effectively reduced by quercetin treatment. Further experiments showed that knockdown of p53 markedly enhanced autophagic activity. In contrast, p53 overexpression substantially counteracted the autophagy-restorative effects induced by quercetin. Collectively, these

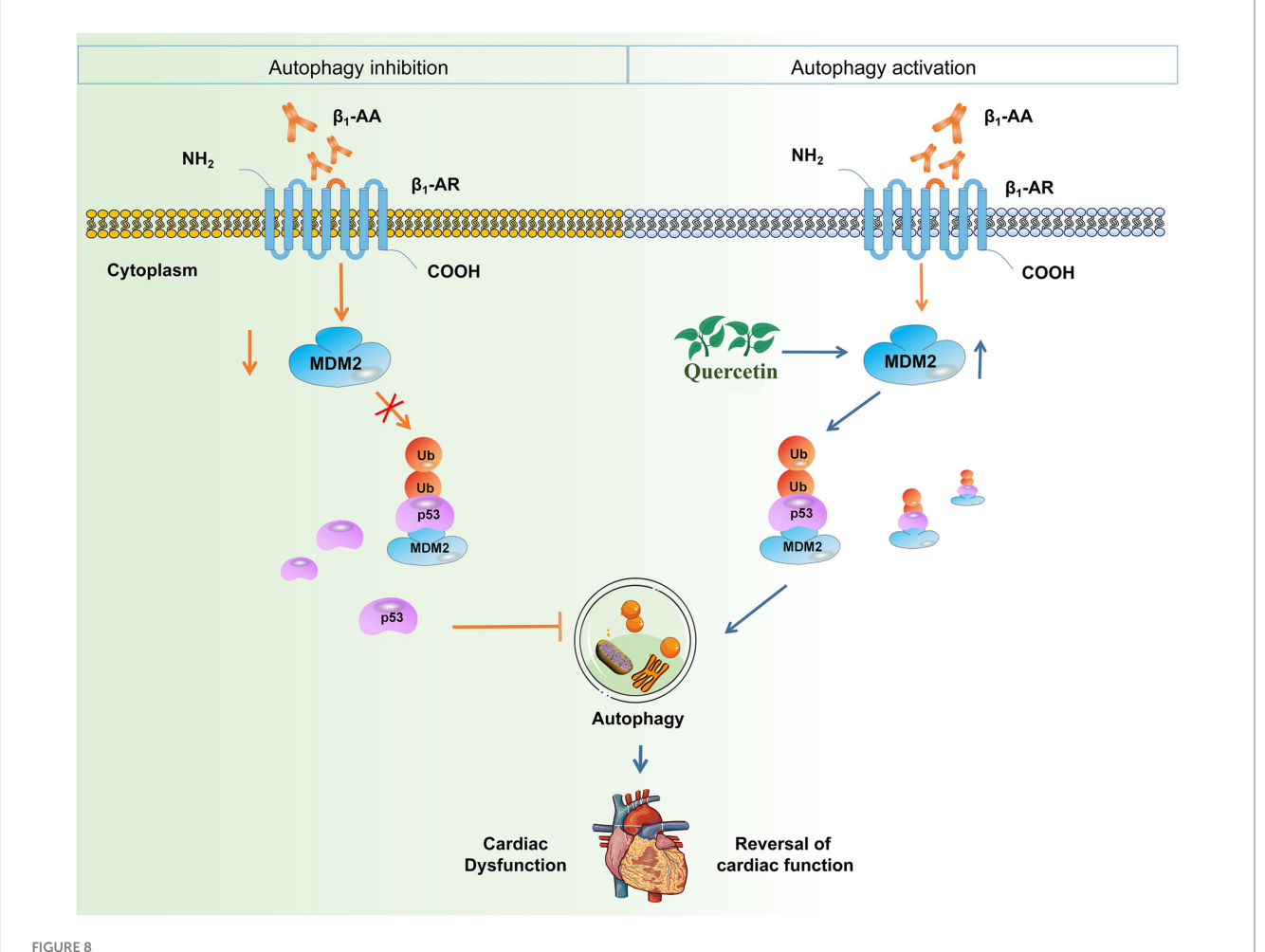
findings indicated that quercetin reverses  $\beta_1$ -AA-induced autophagy inhibition in a p53-dependent manner. Moreover, we observed that while quercetin treatment significantly decreased p53 protein levels, it did not alter p53 mRNA levels. This suggests that quercetin does not regulate p53 expression at the transcriptional level; instead, it may increase degradation of the p53 protein. p53 regulation is mainly dependent on the control of protein stability (50). To explore the mechanism of p53 degradation, we used R packages to analyze the targets of quercetin and found significant enrichment in the



Ouercetin reverses MDM2 protein downregulation in myocardial tissue induced by  $\beta_1$ -AA. (A) Binding sites and hydrogen bonds between quercetin and MDM2. (B) RMSD of quercetin and MDM2. (C) Distribution of SSEs within MDM2, according to residue index. (D) Trajectory of SSE evolution and residue participation in SSEs. (E) RMSF of MDM2 and quercetin. (F) 2D structure of the interaction region. (G) Distribution of interaction bonds and their formation frequency. (H) Trajectory of the total interactions and participating amino acids per frame. (I) Western blot analysis of MDM2 protein levels in C57BL/6 mice actively immunized with  $\beta_1$ -AR-ECII peptide segment for 4 weeks and treated with quercetin (n = 4). (J) Western blot analysis of MDM2 protein levels in H9c2 cardiomyocytes after 4 h of quercetin pre-treatment followed by 24 h of  $\beta_1$ -AA treatment (n = 6). (K,L) Statistical analysis of MDM2 levels. (M) MDM2 mRNA levels after 4 h of quercetin pre-treatment and 24 h of  $\beta_1$ -AA treatment, as determined by RT-PCR (n = 3). (N) Western blotting analysis of LC3 and p62 protein levels after treatment with the MDM2-specific inhibitor Nutlin-3a, following quercetin reversal of  $\beta_1$ -AA-induced changes (n = 6). (O,P,Q) Statistical charts for p53, LC3, and p62 protein expression levels. Data are presented as mean  $\pm$  SD. \*\*p < 0.001, \*\*\*p < 0.001 vs. Ctrl; \*p < 0.05, \*\*p < 0.01 vs.  $\beta_1$ -AA group; \*p < 0.001, \*p < 0.001 vs. Ctrl; \*p < 0.001 vs. p < 0.001 vs. p

ubiquitination degradation pathway. Ubiquitination, a crucial post-translational modification, is closely related to cardiovascular diseases (51). We then used Co-IP to assess p53 ubiquitination levels and found that quercetin indeed reversed the decline in p53 ubiquitination levels induced by  $\beta_1$ -AA, thus normalizing p53 protein expression. To

further investigate the mechanism of p53 ubiquitination and degradation, we performed molecular docking between p53 and the classical E3 ubiquitin ligase MDM2. The results indicated a binding affinity of < 6.9 kcal·mol<sup>-1</sup>. Experimental validation confirmed that  $\beta_1$ -AA reduces MDM2 protein levels, while quercetin restored MDM2



Quercetin alleviates  $\beta_1$ -AA-induced HF by enhancing autophagy via the MDM2/p53 pathway. This study demonstrates that quercetin counteracts  $\beta_1$ -AA-induced HF. The core mechanism involves quercetin upregulating MDM2 expression, which promotes the ubiquitination and degradation of p53. This subsequently relieves the inhibitory effect of p53 on cardiomyocyte autophagy, ultimately restoring autophagic flux and conferring cardioprotection.

expression. Furthermore, the MDM2-specific inhibitor Nutlin-3a diminished the effect of quercetin on p53 protein degradation and weakened the ability of quercetin to reverse the  $\beta_1$ -AA-induced decline in autophagy levels. This confirmed that quercetin increased MDM2 expression in cardiomyocytes, which mediated p53 ubiquitination and degradation, thus reversing the  $\beta_1$ -AA-induced decline in autophagy levels.

### 5 Conclusion

In conclusion, our study unveils a novel cardioprotective mechanism of quercetin against  $\beta_1$ -AA-induced HF. We definitively established that quercetin alleviates HF by restoring impaired myocardial autophagy. The core finding is that quercetin achieves this effect by targeting the p53 protein. Specifically, we identified that quercetin promotes the MDM2-mediated ubiquitination and degradation of p53, which reverses the autophagy suppression caused by  $\beta_1$ -AA (Figure 8). These findings not only elucidate a new molecular pathway through which quercetin exerts its therapeutic effects but also

provide a solid experimental foundation for targeting the p53-MDM2-autophagy axis as a promising strategy for treating autoimmune-related heart failure.

### Data availability statement

Publicly available datasets were analyzed in this study. This data can be found here: https://www.ncbi.nlm.nih.gov/geo/, accession numbers GSE57338, GSE5406, and GSE3586.

### Ethics statement

The animal study was approved by All animal experiments were performed in strict compliance with the ARRIVE guidelines and relevant regulations, with protocols approved by the Experimental Animal Ethics Committee of Shanxi Medical University. The study was conducted in accordance with the local legislation and institutional requirements.

### **Author contributions**

MM: Conceptualization, Methodology, Validation, Writing – original draft, Writing – review & editing. XJ: Validation, Writing – original draft. WL: Visualization, Writing – original draft. JX: Formal analysis, Writing – original draft. YY: Investigation, Writing – review & editing. XZ: Formal analysis, Writing – original draft. JF: Software, Writing – original draft. YLo: Conceptualization, Writing – original draft. YLi: Formal analysis, Writing – original draft. ZZ: Resources, Writing – original draft. XW: Project administration, Writing – original draft. LW: Funding acquisition, Supervision, Writing – review & editing, Writing – original draft.

### **Funding**

The author(s) declare that financial support was received for the research and/or publication of this article. This work was supported by the Basic Research Project of the Shanxi Science and Technology Department (No. 202303021221134), National Natural Science Foundation of China (No. 31871177; No. 82271523), Shanxi Province Higher Education "Billion Project" Science and Technology Guidance Project (No. BYJL034), Central Guiding Local Science and Technology Development Fund Projects (YDZJSX20231A053).

### Acknowledgments

This study utilized publicly available data from the GEO database. We acknowledge the researchers who made these datasets available.

### References

- 1. Jiang Y, Gu J, Niu X, Hu J, Zhang Y, Li D, et al. Phosphorylation-regulated dynamic phase separation of HIP-55 protects against heart failure. *Circulation*. (2024) 150:938–51. doi: 10.1161/CIRCULATIONAHA.123.067519
- 2. Wang L, Hao H, Wang J, Wang X, Zhang S, Du Y, et al. Decreased autophagy: a major factor for cardiomyocyte death induced by  $\beta_1$ -adrenoceptor autoantibodies. *Cell Death Dis.* (2015) 6:e1862. doi: 10.1038/cddis.2015.237
- 3. Holthoff H-P, Zeibig S, Jahns-Boivin V, Bauer J, Lohse MJ, Kääb S, et al. Detection of anti- $\beta_1$ -AR autoantibodies in heart failure by a cell-based competition ELISA. *Circ Res.* (2012) 111:675–84. doi: 10.1161/CIRCRESAHA.112.272682
- 4. Düngen H-D, Dordevic A, Felix SB, Pieske B, Voors AA, McMurray JJV, et al.  $\beta_1$ -adrenoreceptor autoantibodies in heart failure: physiology and therapeutic implications. *Circ Heart Fail.* (2020) 13:e006155. doi: 10.1161/CIRCHEARTFAILURE.119.006155
- 5. Störk S, Boivin V, Horf R, Hein L, Lohse MJ, Angermann CE, et al. Stimulating autoantibodies directed against the cardiac beta1-adrenergic receptor predict increased mortality in idiopathic cardiomyopathy. *Am Heart J.* (2006) 152:697–704. doi: 10.1016/j.ahj.2006.05.004
- 6. Arriola Apelo SI, Lamming DW. Rapamycin: An InhibiTOR of aging emerges from the soil of Easter Island. *J Gerontol A Biol Sci Med Sci.* (2016) 71:841–9. doi: 10.1093/gerona/glw090
- 7. Hao P, Jiang F, Cheng J, Ma L, Zhang Y, Zhao Y. Traditional Chinese medicine for cardiovascular disease: evidence and potential mechanisms. *J Am Coll Cardiol.* (2017) 69:2952–66. doi: 10.1016/j.jacc.2017.04.041
- 8. Sun J, Zhang K, Xiong W-J, Yang G-Y, Zhang Y-J, Wang C-C, et al. Clinical effects of a standardized Chinese herbal remedy, Qili Qiangxin, as an adjuvant treatment in heart failure: systematic review and meta-analysis. *BMC Complement Altern Med.* (2016) 16:201. doi: 10.1186/s12906-016-1174-1
- 9. Cheang I, Yao W, Zhou Y, Zhu X, Ni G, Lu X, et al. The traditional Chinese medicine Qiliqiangxin in heart failure with reduced ejection fraction: a randomized, double-blind, placebo-controlled trial. *Nat Med.* (2024) 30:2295–302. doi: 10.1038/s41591-024-03169-2

### Conflict of interest

The authors declare that the research was conducted in the absence of any commercial or financial relationships that could be construed as a potential conflict of interest.

### Generative AI statement

The authors declare that no Gen AI was used in the creation of this manuscript.

Any alternative text (alt text) provided alongside figures in this article has been generated by Frontiers with the support of artificial intelligence and reasonable efforts have been made to ensure accuracy, including review by the authors wherever possible. If you identify any issues, please contact us.

### Publisher's note

All claims expressed in this article are solely those of the authors and do not necessarily represent those of their affiliated organizations, or those of the publisher, the editors and the reviewers. Any product that may be evaluated in this article, or claim that may be made by its manufacturer, is not guaranteed or endorsed by the publisher.

### Supplementary material

The Supplementary material for this article can be found online at: https://www.frontiersin.org/articles/10.3389/fnut.2025.1674507/full#supplementary-material

- 10. He L, Liu Y, Yang K, Zou Z, Fan C, Yao Z, et al. The discovery of Q-markers of Qiliqiangxin capsule, a traditional Chinese medicine prescription in the treatment of chronic heart failure, based on a novel strategy of multi-dimensional "radar chart" mode evaluation. *Phytomedicine*. (2021) 82:153443. doi: 10.1016/j.phymed.2020.153443
- 11. Ye Y, Gong H, Wang X, Wu J, Wang S, Yuan J, et al. Combination treatment with antihypertensive agents enhances the effect of Qiliqiangxin on chronic pressure overload-induced cardiac hypertrophy and Remodeling in male mice. *J Cardiovasc Pharmacol.* (2015) 65:628–39. doi: 10.1097/FJC.0000000000000230
- 12. Chang X, Zhang T, Meng Q, Wang S, Yan P, Wang X, et al. Quercetin improves cardiomyocyte vulnerability to hypoxia by regulating SIRT1/TMBIM6-related mitophagy and endoplasmic reticulum stress. *Oxidative Med Cell Longev.* (2021) 2021:5529913. doi: 10.1155/2021/5529913
- 13. Hu J, Wang X, Cui X, Kuang W, Li D, Wang J. Quercetin prevents isoprenaline-induced myocardial fibrosis by promoting autophagy via regulating miR-223-3p/FOXO3. *Cell Cycle*. (2021) 20:1253–69. doi: 10.1080/15384101.2021.1932029
- 14. Taminau J, Meganck S, Lazar C, Steenhoff D, Coletta A, Molter C, et al. Unlocking the potential of publicly available microarray data using *in silico* Db and *in silico* merging R/Bioconductor packages. *BMC Bioinformatics*. (2012) 13:335. doi: 10.1186/1471-2105-13-335
- 15. Johnson WE, Li C, Rabinovic A. Adjusting batch effects in microarray expression data using empirical bayes methods. *Biostatistics*. (2007) 8:118–27. doi: 10.1093/biostatistics/kxj037
- 16. Ritchie ME, Phipson B, Wu D, Hu Y, Law CW, Shi W, et al. Limma powers differential expression analyses for RNA-sequencing and microarray studies. *Nucleic Acids Res.* (2015) 43:e47. doi: 10.1093/nar/gkv007
- 17. Wu T, Hu E, Xu S, Chen M, Guo P, Dai Z, et al. Clusterprofiler 4.0: a universal enrichment tool for interpreting omics data. *Innovation (Camb)*. (2021) 2:100141. doi: 10.1016/j.xinn.2021.100141

- 18. Ru J, Li P, Wang J, Zhou W, Li B, Huang C, et al. TCMSP: a database of systems pharmacology for drug discovery from herbal medicines. *J Cheminform*. (2014) 6:13. doi: 10.1186/1758-2946-6-13
- 19. Xu X, Zhang W, Huang C, Li Y, Yu H, Wang Y, et al. A novel chemometric method for the prediction of human oral bioavailability. *Int J Mol Sci.* (2012) 13:6964–82. doi: 10.3390/iims13066964
- 20. Yang S, Zhang J, Yan Y, Yang M, Li C, Li J, et al. Network pharmacology-based strategy to investigate the pharmacologic mechanisms of *Atractylodes macrocephala* Koidz. For the treatment of chronic gastritis. *Front Pharmacol.* (2019) 10:1629. doi: 10.3389/fphar.2019.01629
- 21. Zhou Y, Zhang Y, Zhao D, Yu X, Shen X, Zhou Y, et al. TTD: therapeutic target database describing target druggability information. *Nucleic Acids Res.* (2024) 52:D1465–77. doi: 10.1093/nar/gkad751
- 22. Piñero J, Saüch J, Sanz F, Furlong LI. The DisGeNET cytoscape app: exploring and visualizing disease genomics data. *Comput Struct Biotechnol J.* (2021) 19:2960–7. doi: 10.1016/j.csbj.2021.05.015
- 23. Wishart DS, Feunang YD, Guo AC, Lo EJ, Marcu A, Grant JR, et al. DrugBank 5.0: a major update to the DrugBank database for 2018. *Nucleic Acids Res.* (2018) 46:D1074–82. doi: 10.1093/nar/gkx1037
- 24. Chin C-H, Chen S-H, Wu H-H, Ho C-W, Ko M-T, Lin C-Y. cytoHubba: identifying hub objects and sub-networks from complex interactome. *BMC Syst Biol.* (2014) 8:S11. doi: 10.1186/1752-0509-8-S4-S11
- 25. Szklarczyk D, Gable AL, Nastou KC, Lyon D, Kirsch R, Pyysalo S, et al. The STRING database in 2021: customizable protein-protein networks, and functional characterization of user-uploaded gene/measurement sets.  $Nucleic\ Acids\ Res.\ (2021)\ 49:D605–12.\ doi: 10.1093/nar/gkaa1074$
- 26. Berman HM, Westbrook J, Feng Z, Gilliland G, Bhat TN, Weissig H, et al. The protein data Bank. *Nucleic Acids Res.* (2000) 28:235–42. doi: 10.1093/nar/28.1.235
- 27. Morris GM, Huey R, Lindstrom W, Sanner MF, Belew RK, Goodsell DS, et al. AutoDock4 and AutoDockTools4: automated docking with selective receptor flexibility. *J Comput Chem.* (2009) 30:2785–91. doi: 10.1002/jcc.21256
- 28. Seeliger D, de Groot BL. Ligand docking and binding site analysis with PyMOL and autodock/vina. *J Comput Aided Mol Des.* (2010) 24:417–22. doi: 10.1007/s10822-010-9352-6
- 29. Zhi X, Shi S, Li Y, Ma M, Long Y, Li C, et al. S100a9 inhibits Atg9a transcription and participates in suppression of autophagy in cardiomyocytes induced by  $\beta$ (1)-adrenoceptor autoantibodies. Cell Mol Biol Lett. (2023) 28:74. doi: 10.1186/s11658-023-00486-1
- 30. Wang L, Tan A, An X, Xia Y, Xie Y. Quercetin dihydrate inhibition of cardiac fibrosis induced by angiotensin II *in vivo* and *in vitro*. *Biomed Pharmacother*. (2020) 127:110205. doi: 10.1016/j.biopha.2020.110205
- 31. Sun C, Lu J, Long Y, Guo S, Jia W, Ning N, et al. Adiponectin up-regulates the decrease of myocardial autophagic flux induced by  $\beta_1$  -adrenergic receptor autoantibody partly dependent on AMPK. *J Cell Mol Med.* (2021) 25:8464–78. doi: 10.1111/jcmm.16807
- 32. Nag S, Mitra O, Maturi B, Kaur SP, Saini A, Nama M, et al. Autophagy and mitophagy as potential therapeutic targets in diabetic heart condition: harnessing the power of nanotheranostics. *Asian J Pharm Sci.* (2024) 19:100927. doi: 10.1016/j.ajps.2024.100927
- 33. Nishida K, Kyoi S, Yamaguchi O, Sadoshima J, Otsu K. The role of autophagy in the heart. *Cell Death Differ.* (2009) 16:31–8. doi: 10.1038/cdd.2008.163
- 34. Rothermel BA, Hill JA. Autophagy in load-induced heart disease. *Circ Res.* (2008) 103:1363–9. doi: 10.1161/CIRCRESAHA.108.186551
- 35. Markousis-Mavrogenis G, Baumhove L, Al-Mubarak AA, Aboumsallem JP, Bomer N, Voors AA, et al. Immunomodulation and immunopharmacology in heart failure. *Nat Rev Cardiol.* (2024) 21:119–49. doi: 10.1038/s41569-023-00919-6

- 36. Cao N, Chen H, Bai Y, Yang X, Xu W, Hao W, et al.  $\beta_2$ -adrenergic receptor autoantibodies alleviated myocardial damage induced by  $\beta_1$ -adrenergic receptor autoantibodies in heart failure. *Cardiovasc Res.* (2018) 114:1487–98. doi: 10.1093/cvr/cvy105
- 37. Wallukat G, Müller J, Podlowski S, Nissen E, Morwinski R, Hetzer R. Agonist-like beta-adrenoceptor antibodies in heart failure. *Am J Cardiol.* (1999) 83:75H–9H.
- 38. Jane-wit D, Altuntas CZ, Johnson JM, Yong S, Wickley PJ, Clark P, et al. Beta 1-adrenergic receptor autoantibodies mediate dilated cardiomyopathy by agonistically inducing cardiomyocyte apoptosis. *Circulation*. (2007) 116:399–410. doi: 10.1161/CIRCULATIONAHA.106.683193
- 39. Wang L, Li Y, Ning N, Wang J, Yan Z, Zhang S, et al. Decreased autophagy induced by  $\beta_1$ -adrenoceptor autoantibodies contributes to cardiomyocyte apoptosis. *Cell Death Dis.* (2018) 9:406. doi: 10.1038/s41419-018-0445-9
- 40. Jiao X, Jin X, Ma Y, Yang Y, Li J, Liang L, et al. A comprehensive application: molecular docking and network pharmacology for the prediction of bioactive constituents and elucidation of mechanisms of action in component-based Chinese medicine. *Comput Biol Chem.* (2021) 90:107402. doi: 10.1016/j.compbiolchem.2020.107402
- 41. Leung AYL, Zhang J, Chan CY, Chen X, Mao J, Jia Z, et al. Validation of evidence-based questionnaire for TCM syndrome differentiation of heart failure and evaluation of expert consensus. *Chin Med.* (2023) 18:70. doi: 10.1186/s13020-023-00757-1
- 42. Xing X, Guo J, Mo J, Li H, Zhang H, Shao B, et al. Qili qiangxin capsules for chronic heart failure: a GRADE-assessed clinical evidence and preclinical mechanism. *Front Cardiovasc Med.* (2022) 9:1090616. doi: 10.3389/fcvm.2022.1090616
- 43. Zhou J, Wang Z, He Y, Luo X, Zhang W, Yu L, et al. Qiliqiangxin reduced cardiomyocytes apotosis and improved heart function in infarcted heart through Pink1/parkin -mediated mitochondrial autophagy. *BMC Complement Med Ther*. (2020) 20:203. doi: 10.1186/s12906-020-02992-7
- 44. Tong J, Lai Y, Yao Y-A, Wang X-J, Shi Y-S, Hou H-J, et al. Qiliqiangxin rescues mouse cardiac function by regulating AGTR1/TRPV1-mediated autophagy in STZ-induced diabetes mellitus. *Cell Physiol Biochem.* (2018) 47:1365–76. doi: 10.1159/000490822
- 45. Zhao L, Zhang H, Li N, Chen J, Xu H, Wang Y, et al. Network pharmacology, a promising approach to reveal the pharmacology mechanism of Chinese medicine formula. *J Ethnopharmacol.* (2023) 309:116306. doi: 10.1016/j.jep.2023.116306
- 46. Bappi MH, Mia MN, Ansari SA, Ansari IA, Prottay AAS, Akbor MS, et al. Quercetin increases the antidepressant-like effects of sclareol and antagonizes diazepam in thiopental sodium-induced sleeping mice: a possible GABAergic transmission intervention. *Phytother Res.* (2024) 38:2198–214. doi: 10.1002/ptr.8139
- 47. Ungurianu A, Zanfirescu A, Margină D. Exploring the therapeutic potential of quercetin: a focus on its sirtuin-mediated benefits. *Phytother Res.* (2024) 38:2361–87. doi: 10.1002/ptr.8168
- 48. Chang X, Zhang T, Wang J, Liu Y, Yan P, Meng Q, et al. SIRT5-related Desuccinylation modification contributes to quercetin-induced protection against heart failure and high-glucose-prompted cardiomyocytes injured through regulation of mitochondrial quality surveillance. Oxidative Med Cell Longev. (2021) 2021:5876841. doi: 10.1155/2021/5876841
- 49. Li H, Li C, Zhai W, Zhang X, Li L, Wu B, et al. Destabilization of TP53 by USP10 is essential for neonatal autophagy and survival. *Cell Rep.* (2022) 41:111435. doi: 10.1016/j.celrep.2022.111435
- 50. Yan H, Wu W, Hu Y, Li J, Xu J, Chen X, et al. Regorafenib inhibits EphA2 phosphorylation and leads to liver damage via the ERK/MDM2/p53 axis. *Nat Commun*. (2023) 14:2756. doi: 10.1038/s41467-023-38430-8
- 51. Zhang Y, Qian H, Wu B, You S, Wu S, Lu S, et al. E3 ubiquitin ligase NEDD4 family-regulatory network in cardiovascular disease. *Int J Biol Sci.* (2020) 16:2727–40. doi: 10.7150/ijbs.48437

### Glossary

 $\pmb{\beta_1\text{-}AA}$  -  $\beta_1\text{-}adrenergic$  receptor autoantibody

 $\beta_1$ -AR -  $\beta_1$ -adrenergic receptor

SA - Streptavidin

ECII - Second extracellular loop

TCMSP - Traditional Chinese Medicine Systems

Pharmacology Database

OB - Oral bioavailability

DL - Druglikeness

GEO - Gene expression omnibus

DEGs - Differentially expressed genes

**BSA** - Bovine serum albumin

DMEM - Dulbecco's modified eagle medium

PBS - phosphate-buffered saline

DAPI - 4',6-diamidino-2-phenylindole

**QUE** - Quercetin

p53 - Tumor protein P53

MDM2 - Murine double minute2

Co-IP - Co-immunoprecipitation

FS - Fractional shortening

**EF** - Ejection fraction

 $\ensuremath{\textbf{LVIDs}}$  - Left ventricular end-systolic diameter

LVIDd - Left ventricular end-diastolic diameter

ESV - End-systolic volume

EDV - End-diastolic volume